Biochimica et Biophysica Acta 1840 (2014) 80–85

Contents lists available at ScienceDirect

Biochimica et Biophysica Acta

journal homepage: www.elsevier.com/locate/bbagen

Expanding the paradigm of thiol redox in the thermophilic root of life

Joshua Heinemann [a], Timothy Hamerly [a], Walid S. Maaty [a], Navid Movahed [a], Joseph D. Steffens [a], Benjamin D. Reeves [a], Jonathan K. Hilmer [b], Jesse Therien [a,c], Paul A. Grieco [a], John W. Peters [a,c], Brian Bothner [a,b,*]

[a] Department of Chemistry and Biochemistry, Montana State University, Bozeman, MT 59717, USA
[b] Mass Spectrometry, Proteomics and Metabolomics Core Facility, Montana State University, Bozeman, MT 59717, USA
[c] Thermal Biology Institute, Montana State University, Bozeman, MT 59717, USA

ARTICLE INFO

Article history:
Received 13 June 2013
Received in revised form 7 August 2013
Accepted 11 August 2013
Available online 17 August 2013

Keywords:
Thiol
Glutathione
Thermophile
Disulfide
Proteomics
Metabolomics

ABSTRACT

Background: The current paradigm of intracellular redox chemistry maintains that cells establish a reducing environment maintained by a pool of small molecule and protein thiol to protect against oxidative damage. This strategy is conserved in mesophilic organisms from all domains of life, but has been confounded in thermophilic organisms where evidence suggests that intracellular proteins have abundant disulfides.
Methods: Chemical labeling and 2-dimensional gel electrophoresis were used to capture disulfide bonding in the proteome of the model thermophile *Sulfolobus solfataricus*. The redox poise of the metabolome was characterized using both chemical labeling and untargeted liquid chromatography mass spectrometry. Gene annotation was undertaken using support vector machine based pattern recognition.
Results: Proteomic analysis indicated the intracellular protein thiol of *S. solfataricus* was primarily in the disulfide form. Metabolic characterization revealed a lack of reduced small molecule thiol. Glutathione was found primarily in the oxidized state (GSSG), at relatively low concentration. Combined with genetic analysis, this evidence shows that pathways for synthesis of glutathione do exist in the archaeal domain.
Conclusions: In observed thermophilic organisms, thiol abundance and redox poise suggest that this system is not directly utilized for protection against oxidative damage. Instead, a more oxidized intracellular environment promotes disulfide bonding, a critical adaptation for protein thermostability.
General significance: Based on the placement of thermophilic archaea close to the last universal common ancestor in rRNA phylogenies, we hypothesize that thiol-based redox systems are derived from metabolic pathways originally tasked with promoting protein stability.

1. Introduction

Intracellular oxidation–reduction potential must be carefully balanced to support oxidative metabolic processes, while protecting from detrimental effects of free radical damage. It is generally accepted that the cytoplasm is kept in a reducing (electron rich) state, with small variations between different cell types [1]. The cytoplasmic redox potential is typically quantified by measuring relative amounts of protein disulfide (PSSP) to thiol (PSH) in equilibrium with compounds of known redox potential, such as oxidized (GSSG) and reduced glutathione (GSH) [2–5]. In the cytoplasm of eukaryotic and most gram negative prokaryotes, GSH and PSH are the predominant forms and exist at significant concentrations [5–7]. Whereas, GSSG and PSSP are primarily present in more oxidizing environments, such as extracellular space, mitochondria [4,8–10] or as catalytic intermediates.

In contrast, structural and genomic evidence suggests thermophiles and their viruses favor higher ratios of PSSP to PSH. The abundance of PSSP is proposed to be an adaptation that increases protein stability at elevated temperatures [11,12]. The genomic analyses show that this adaptation is exclusive to thermophilic organisms, with the highest proposed PSSP/PSH ratios observed in the hyperthermophilic Crenarchaea [12–17]. *Sulfolobus solfataricus* is a hyperthermophilic Crenarchaeon living optimally at 80 °C and a pH of 3, and has been adopted as a model for study of high temperature adaptation [18–24]. Previous studies of *S. solfataricus* and phylogenetically related thermophiles failed to find glutathione [25,26], raising the question, how do these organisms regulate intracellular redox and protein disulfide formation? Organisms without glutathione typically have an alternative small molecule thiol fulfilling this role [6,25–27]; however both proteomic and genomic evidence have failed to provide evidence of common thiol-biosynthesis pathways in *S. solfataricus* and its thermophilic relatives [14,25].

The maintenance of thiol redox homeostasis is fundamentally important to an organism's ability to protect against oxidative damage. PSSP/PSH and GSSG/GSH ratios are often used as a proxy for estimating intracellular redox state and tracking changes [2–5]. *S. Solfataricus*

* Corresponding author at: 126 Chemistry Biochemistry Bldg., Bozeman, MT 59717, USA. Tel.: +1 406 994 5270.
E-mail address: bbothner@chemistry.montana.edu (B. Bothner).

0304-4165/$ – see front matter © 2013 Elsevier B.V. All rights reserved.
http://dx.doi.org/10.1016/j.bbagen.2013.08.009

utilizes a novel enzyme system for regulating oxidative stress [22,28], but no evidence supports the role of intracellular thiol in this process. Herein we provide evidence that both metabolites and proteins of *S. solfataricus* are tuned to operate in a noncanonical redox environment. We find that *S. solfataricus* does utilize glutathione, although primarily in the oxidized form. Because the balance of oxidized to reduced protein and small molecule thiol is tilted toward oxidized PSSP and GSSG, this strongly suggests a more oxidized intracellular environment. Together these results characterize a phenotype which lies outside the traditional paradigm, and provides an expanded model of redox homeostasis in thermophilic organisms.

2. Materials and methods

2.1. Growth of microorganisms

S. solfataricus P2 (ATCC) was grown aerobically in liquid DSMZ media 182 (22.78 mM KH_2PO_4, 18.90 mM $(NH_4)_2SO_4$, 0.81 mM $MgSO_4$, 1.7 mM $CaCl_2$, 0.2% Yeast Extract) (Media 1), or with the addition of 0.1% glucose as carbon source (Media 2), pH adjusted to 2.8 with 6 M H_2SO_4. Media was analyzed to ensure no glutathione or small molecule contaminant affected results. Batch cultures of *S. solfataricus* were grown with media in long neck Erlenmeyer flasks at 80 °C. One liter of media was inoculated with 10 ml of log phase (OD_{650} 0.33) culture and divided evenly between ten, 1-liter long neck flasks. At (OD_{650}, 0.35), 50 ml of each 0.25 liter culture was removed and placed in a 50 ml falcon tube as growth controls. Cells were collected at exponential, late exponential and stationary growth phases for metabolite extraction. Liquid cultures of recombinant *Escherichia coli* (Strain: BL21-D3) were grown in Luria-Bertani media (1% Peptone, 0.5% Yeast Extract and 1% NaCl, pH = 7) in 1 l shaker flasks at 37 °C. For oxidative stress experiment, H_2O_2 was administered to a final concentration of 30 μM (n = 10). One liter of media was inoculated with 10 ml of log phase (OD_{650} 0.33) *S. solfataricus* culture and divided evenly between four, 1-liter long neck flasks. At (OD_{650}, 0.35), 50 ml of each 0.25 liter culture was removed and placed in a 50 ml falcon tube as stressed growth controls. An additional 50 ml aliquot was collected from each culture at 30 min post H_2O_2 inoculation and used for metabolite extraction.

2.2. Zdye maleimide probes for thiol labeling

Cells were lysed with combination of freeze/thaw cycles. Protein sample extracts were prepared from cell suspensions in ice cold, phosphate buffer solution (pH = 6.5, 1 mM EDTA). All buffers were degassed and kept on ice during extraction to help ensure lack of thiol/disulfide exchange. Proteins were purified and concentrated with 5-fold volume of cold acetone (−80 °C). Protein concentration was measured with RC/DC Protein Assay Kit (Bio-Rad). For each experiment, 50 μg of protein was used. Three replicates were reduced using 20 mM tributylphosphine (Sigma) for 20 min at room temperature, alongside three unreduced controls. Dye labeling was performed using a fluorescent Zdye (Blue emitting ZB-M LC-01-56, and Green emitting BDR-III-172) coupled to a maleimide, in a method modified from [23]. Dye was added to a final concentration of 5 μM in PBS, pH 6.5, for 20 min at room temperature. Reactions were quenched with 5-fold excess acetone (−80 °C). Samples were centrifuged at 15,000 ×*g* and the protein pellet was resuspended in 2D gel-loading buffer containing 40 mM DTT. Total protein internal standards were labeled with Cy5 DIGE flor using minimal labeling methods according to the manufacturer's protocol (GE Healthcare). 50 μg of protein extract was labeled at 0 °C in the dark for 30 min with 400 pmoles of Cy5 DIGE flor dissolved in 99.8% DMF (Sigma). Labeling reactions were quenched by the addition of 1 μl of a 10 mM L-lysine solution (Sigma) and left on ice for 10 min. Cy5, reduced and unreduced Zdye samples (ZB-M LC-01-56) were combined appropriately and mixed with rehydration buffer (7 M urea, 2 M thiourea, 4% CHAPS). 2-DE was performed as described elsewhere [23] using precast IPG strips (pH 3–11 NL, 24 cm length; GE Healthcare) in the first dimension (IEF). Labeled samples were combined with a maximum of 450 μl of rehydration buffer (7 M urea, 2 M thiourea, 4% CHAPS, 0.5% IPG buffer pH = 3–11 NL, 40 mM DTT, and a trace of bromophenol blue) and loaded onto IPG strips. 150 μg of protein was loaded onto each strip and IEF was carried out with the IPGPhor II (GE Healthcare). Focusing was carried out at 20 °C with a maximum of 50 μA/strip. Active rehydration was achieved by applying 50 V for 12 h. This was followed by a stepwise progression of 500 V for 500 Vh, gradient ramp from 500 to 1000 V for 1 h, gradient ramp from 3000 to 5000 V for 1 h, gradient ramp from 5000 to 8000 V for 1 h, the 8000 V constant for 44,000 Vh. After IEF separation, the strips were equilibrated twice for 15 min with 50 mM Tris–HCl, 6 M Urea, 30% glycerol, 2% SDS and a trace of bromophenol blue, pH 8.8). The first equilibration solution contained 65 mM DTT, and the second 150 mM iodoacetamide. The strips were sealed on the top of the gels using a sealing solution (0.75% agarose in SDS-Tris–HCl buffer). The second-dimension SDS-PAGE was performed in a Dalt II (GE Healthcare), using 1 mm thick, 24-cm, 13% polyacrylamide gels, and electrophoresis were carried out at a constant current (45 min at 2 W/gel, then at 1 W/gel for ~16 h at 25 °C). 2D gels were scanned on a Typhoon Trio Imager according to manufacturer's protocol (GE Healthcare) at 100 μm resolution with excitation wavelength of 532 nm with a long pass emission wavelength of 580 nm and 488 nm with 520 nm emission for Zdyes, and 633 nm with long pass emission of 670 nm for Cy5 DIGE flor. The number of visible protein spots was counted for direct comparison; fluorescent measurements and image processing was done using ImageJ [29].

2.3. Metabolite extraction

A survey of the *S. solfataricus* metabolome was done by extracting metabolites using 60% aqueous (v/v) EtOH, 50% aqueous (v/v) MeOH or MeOH/Chloroform (1 mM EDTA) solvents in an effort to ensure global coverage. Chloroform methanol extraction was a modification from [30]. Briefly, cell pellets were resuspended in 1.5 ml of cold MeOH and transferred to glass tubes, after which 1.5 ml of cold chloroform was added. All samples were then shaken at 0 °C for 2 h using a custom made orbital shaker. The samples were then centrifuged (2000 ×*g*, 15 min, −9 °C). Upper MeOH/chloroform layer was removed and 50% aqueous MeOH (v/v) was added to cellular debris and vortexed for 30 s. After centrifugation the upper phase was pooled with the first extracts. Proteins were precipitated using 5:1 dilution with −80 °C acetone and centrifuged. Upper phase was collected and subsequently dried and resuspended in 50% MeOH. MeOH/H_2O and EtOH/H_2O extraction was a modification from [31]. Briefly each sample was resuspended in 1.5 ml 60% aqueous EtOH or 50% MeOH (v/v) respectively, 1 mM EDTA, vortexed for 30s, and sample was frozen in liquid nitrogen and thawed to room temperature three times. Samples were subsequently sonicated 60% duty cycle maximum power level for 5 min on ice. The sample was incubated 1 h at −20 °C followed by a 15 min centrifugation at 13,000 ×*g* and supernatant was pooled. Cell debris was subsequently washed with 1 ml extraction solvent, vortexed for 30 s and centrifuged. Proteins were precipitated using 5:1 dilution with −80C acetone and centrifuged. Upper phase was collected and subsequently dried and resuspended in 50% MeOH. *Ignicoccus hospitalis* and *E. coli* metabolites were extracted using identical 50% MeOH method.

2.4. LCMS based metabolome analysis

Analyses were performed using a 1290 UPLC coupled to a 6538 UHD Accurate-Mass Q-TOF (Agilent Technologies). The system was operated in positive and negative electrospray ionization modes. Vials containing extracted metabolites and standard mixtures were kept at −80 °C prior to LCMS analysis. Metabolites were separated using a reverse-phase Kinetix 1.7 μm C18, 100A, 150 mm × 2.1 mm (Reverse Phase), or a Cogent Diamond Hydride, 150 mm (HILIC). In positive ionization mode, A = 0.1% formic acid in water B = 0.1% formic acid in acetonitrile. For

negative ionization mode two pairs of solvent systems were used, A1 = 0.1% formic acid in water B1 = 0.1% formic acid in acetonitrile and A2 = 1 mM ammonium fluoride in water B2 = acetonitrile. The C18 linear gradient was 100% A (0–2 min)–100% B with an injection volume of 15 μl. HILIC linear gradient was 5% A (0–2 min)–50% A with an injection volume of 2 μl. ESI conditions were modified from [25] gas temperature 250 °C, drying gas of 12 l/min, nebulizer 30 psig, fragmentor 120 V, and skimmer 65 V. The instrument was set to acquire over the m/z range 50–1000 with an acquisition of 1 spectrum/s. MSMS fragmentation was performed in targeted mode, and the instrument was set to acquire over the m/z range 50–1000, with default isowidth, collision energy was 10–20 V. Data was visualized using MassHunter software package (Agilent Technologies) and data processing was done using XCMS software and XCMS online, small molecule characterizations were done using the Metlin database [32–36].

2.5. GSH labeling and GSSG reduction

A method for labeling reduced glutathione with N-(2-aminoethyl) maleimide was developed using a GSH standard (Sigma) in aqueous methanol (50%, pH 6.5). Using HILIC chromatography described above, a characteristic mass and retention time shift allowed semi-quantitative analysis of labeling to be performed. To test the reaction conditions that were developed, 100 nmol GSH was mixed with 35, 70, and 140 nmol of N-(2-aminoethyl) maleimide in which a linear reduction of GSH and linear accumulation of product was observed (Supplementary Fig. 4A). Metabolite extracts from *S. solfataricus* and *E. coli* were then spiked with 100 nmol N-(2-aminoethyl) maleimide in triplicate and analyzed with XCMS software. Using HILIC methods to visualize GSSG reduction, GSSG standard was spiked into samples (50% MeOH) and reduced, using 10 nmol, 100 nmol and 1 μmol dithioreitol (DTT). Metabolite extracts from *S. solfataricus* were then spiked with 2 μmol DTT in triplicate and analyzed with XCMS software to identify potentially novel small molecule thiols.

2.6. Determination of NADPH-ratio

The intracellular ratio in S. *solfataricus* and *E. coli* (BL21-D3) cells was determined as described by the manufacture of the NADP/NADPH Quantitation Kit, MAK038-1KT (Sigma Inc.). Cells were grown to mid-log and stationary phase, with NADP(H) extracted immediately before measurement.

3. Results

3.1. The S. solfataricus proteome has less cysteine and more disulfide bonds

Genomic analysis revealed that the proteins of *S. solfataricus* have a lower percentage of cysteine than proteins from bacteria (*E. coli*) and eukarya (*Saccharomyces cerevisiae*). Across the proteome of *S. solfataricus* cysteine residues make up only 0.6% of the amino acid composition, compared with 1.2% in *E. coli* and 1.3% in *S. cerevisiae*. In addition, over a third (36.5%) of the proteins from *S. solfataricus* do not contain cysteine, a distinct difference from *E. coli* (15.2%) and *S. cerevisiae* (9.3%).

To determine if a significant fraction of cytosolic proteins in *S. solfataricus* contained oxidized (PSSP), rather than reduced cysteine (PSH), a fluorescent thiol reactive maleimide probe was used to label intracellular proteins. Free cysteine thiols in control and reduced protein extracts were visualized by running the labeled proteins on 2 dimensional gels. The number and intensity of protein spots was substantially increased after reduction (Fig. 1). The increase in reduced thiols after reduction was confirmed by analyzing scanned images of the gels run in triplicate, which showed that average fluorescence intensity increased from 1126 ± 77 relative units in the control, to 1797 ± 282 after reduction. This supports predictions based on sequence analysis, that the intracellular proteins of *S. solfataricus* have an over representation of paired cysteines [11–13].

3.2. The metabolome of S. solfataricus favors oxidized thiol

Results from the analysis of the proteome provide evidence that the intracellular thiol environment of *S. solfataricus* is unlike that reported in all eukaryotes and all but a few prokaryotes. A detailed characterization of the metabolome was undertaken to identify any small molecules involved with maintaining the unusually oxidized PSSP, and find a second indicator of intracellular redox potential. To maximize the metabolic coverage, ultra performance liquid chromatography based mass spectrometry (UPLC/MS) was used to analyze a series of metabolite extractions using multiple solvents (Supplemental Fig. 1). In batch culture, cellular metabolite expression is dependent upon the phase of an organism's growth (Supplemental Fig. 2). Therefore, metabolites from *S. solfataricus* were extracted from cultures grown at mid-log and stationary phases as well as after 30 min of oxidative stress with 30 μM H_2O_2. Untargeted metabolite profiles were compared using both reverse phase and hydrophilic interaction chromatography, to ensure deep coverage (Fig. 2A, B). Analysis of metabolite profiles after 30 min of oxidative stress with 30 μM H_2O_2 allowed visualization of 2065 unique small molecule masses (fold change ≥ 2, p-value ≤ 0.01); none of which matched the mass of common reduced small molecule thiol, such as cysteine, GSH, or Coenzyme A (CoA) (Fig. 2C). CoA was previously suggested as a redox mediator for *S. solfataricus* and related thermophiles [25].

While reduced GSH was not detectable, GSSG was present in low abundance (~12.5 μM) (Fig. 2D). To ensure the lack of appreciable GSH was not caused by the metabolite extraction method, *E. coli* metabolites were extracted from stationary phase using an identical method. GSH was highly abundant. Based upon cell mass and LCMS spectral intensity, the amount of GSSG detected in *S. solfataricus* averaged only

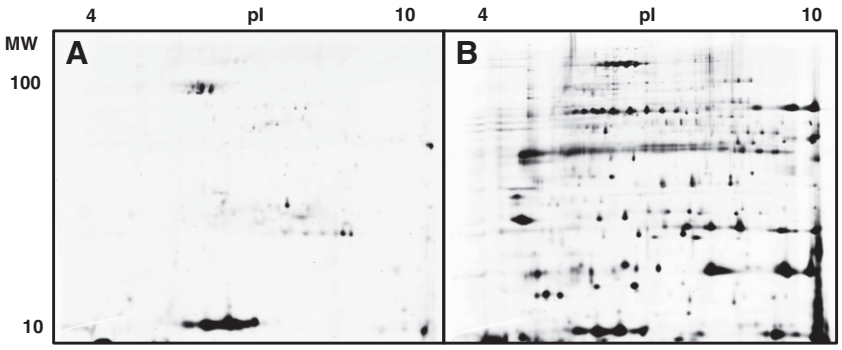

Fig. 1. Cysteine labeling of cytoplasmic proteins of *S. solfataricus* before and after reduction of disulfide bonds. Comparison of reduced thiol content in total protein sample using a fluorescent Zdye-coupled maleimide probe in the native state (A) and after reduction with tributylphosphine (B). The number of proteins labeled and total fluorescence intensity increased after reduction of disulfide bonds.

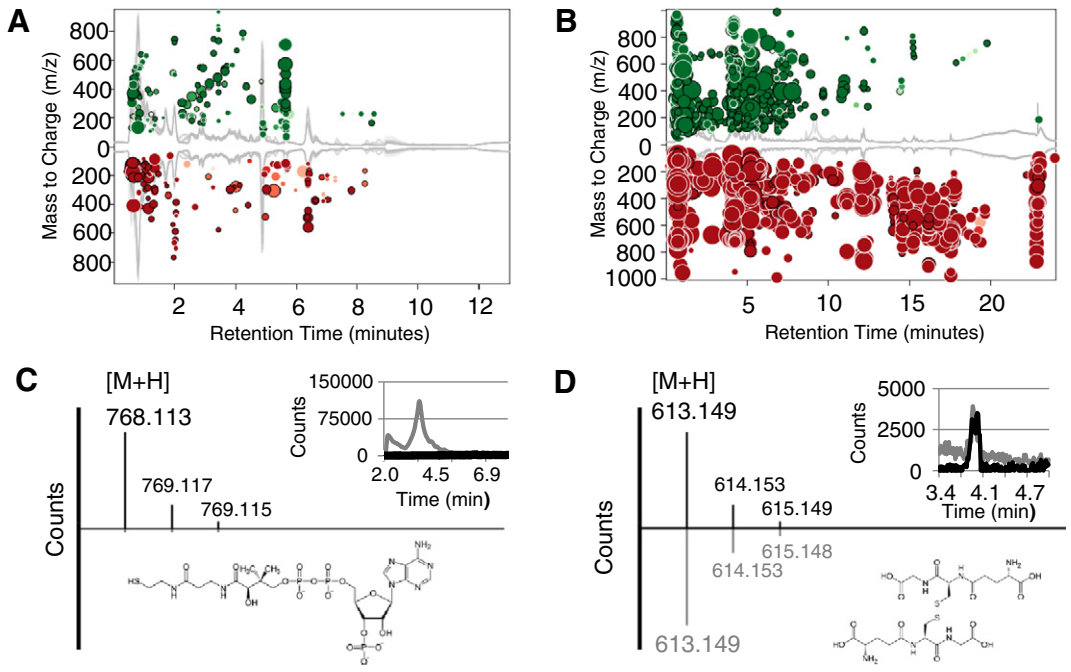

Fig. 2. Metabolic profiling and characterization of thiol content in *S. solfataricus*. A total of 2064 molecular features changed by ≥2-fold, (p-value ≤ 0.01) after 30 min of H_2O_2. Cloud plots of (A) HILIC and (B) reverse-phase show regulated features. Features whose intensity increased are shown on the top in green, whereas those decreased are shown on the bottom in red. Features with lower p-values are brighter. The size of each bubble corresponds to the fold change, as calculated by Welch *t*-test. Plots A and B generated by Metlin online. (C) Lack of CoA in metabolite extracts was confirmed by spike-in experiments which show a clear mass spectrum of CoA standard. Inset, CoA standard (gray), and absence in metabolite extracts (black). (D) Presence of oxidized glutathione (GSSG) in *S. solfataricus*. Mass spectra of GSSG from extract (above) compared to GSSG standard (below). Inset, retention time comparison between GSSG standard (gray) and GSSG in extract (black), structure of GSSG shown for reference.

0.62% (p-value < 0.05) that were found in *E. coli*. Previous reports failed to find glutathione in *S. solfataricus* [25], suggesting that our success may be attributed to the superior sensitivity of UPLC/MS. In most prokaryotic and eukaryotic cells, GSH is typically found in greater abundance than GSSG during normal healthy growth [1]. To further validate this unique redox poise, metabolites from the anaerobic thermophilic archaea *I. hospitalis* were extracted and similar low levels of GSSG were detected, again in the absence of measurable GSH (Supplemental Fig. 3).

3.3. Detection of small molecules using chemical biology

The failure to detect a common reduced small molecule thiol in *S. solfataricus* did not rule out the existence of a novel form, such as that observed in eubacteria and lower temperature thermophilic archaea [26,27]. Therefore, we adopted a chemical labeling approach to search for thiol containing small molecules. The method allows for direct labeling of thiol in cellular extracts using a maleimide reactive group. To test the protocol, reaction of GSH with N-(2-aminoethyl) maleimide was monitored using UPLC/MS. Extracted ion chromatograms (EIC) showed a decrease in substrate and reciprocal accumulation of product (Supplemental Fig. 4A, B), demonstrating that the assay performed as expected. The maleimide probe was then spiked into metabolite extracts from both *S. solfataricus* and *E. coli*. Targeted analysis of *E. coli* extracts showed that native GSH was readily labeled (18-fold reduction, p-value < 0.05) along with several other putatively identified thiols (Table S1), but in the *S. solfataricus* samples, no native reduced thiol reacted with the probe. GSH and N-(2-aminoethyl) maleimide were iteratively spiked into *S. solfataricus* metabolite extract, to validate that there was no unknown interfering small molecule or matrix effects in the extracts. Clear labeling of GSH standard was observed, confirming that if GSH was present at ≥25 μM, it would have been successfully labeled (Supplemental Fig. 5). Glutathione can exist at mM concentrations in eukaryotic mesophiles [7].

To probe the metabolome of *S. solfataricus* for the presence of other oxidized disulfides, a method for reducing oxidized thiols in metabolite extracts was developed. Using this approach GSSG was reduced to GSH by dithiothreitol (DTT) in a dose dependent manner. Differential analysis of the metabolome did not reveal other affected small molecules, strongly supporting a lack of other disulfides. A concentration threshold for the reaction was observed, below which oxidized disulfides could not be reduced. The efficiency of disulfide reduction decayed as the available GSSG concentration decreased (Supplemental Fig. 4C). The inability of DTT to reduce all detectable GSSG in *S. solfataricus*, explains why it would not have been detected previously [25].

3.4. NADPH/$NADP^+$ ratio

NADPH provides reducing equivalents in anabolic pathways and facilitates regeneration of GSH through glutathione reductase [37]. The ratio of NADPH to $NADP^+$ in *S. solfataricus* was determined using a standard colorimetric assay (Sigma Inc.). The results showed that significantly higher levels of oxidized $NADP^+$ were present (Supplemental Fig. 6). While the ratio of oxidized to reduced equivalents of glutathione and NADPH are not directly connected, this provides further evidence that related metabolite pools of *S. solfataricus* maintain a more oxidized potential.

3.5. Genomic justification for GSSG

The experimental evidence indicated GSSG exists in *S. solfataricus*; however, substantial pathway annotation was missing. With the exception of gamma-glutamyl transpeptidase (Sso3216) and disulfide protein oxidoreductase (*Ss*DPO) [9], requisite enzymes for the synthesis of GSH were not known to be present. Updated genome annotation performed by SulfoSYS [20] revealed archaeal clusters of orthologous genes (COG) to glutathione synthase, lactoyl-gluatathione lyase, and glutaredoxin-like proteins. Discovery of GSSG prompted us to investigate these gene clusters further, with the goal of completing the synthetic pathway. While sequence based comparisons often fail when there is high divergence, even low identity can provide evidence of homologous structures and activities [21]. To elucidate the glutathione pathway,

Table 1
Summary of *S. solfataricus* protein with similarity to glutathione synthesis and metabolism.

Gene	arCOG annotation	arCOG #	p-Value
SSO0159	Glutathione synthase/glutaminyl transferase/alpha-L-glutamate ligase	arCOG01589	2.8E−45
SSO0645	Glutathione synthase/glutaminyl transferase/alpha-L-glutamate ligase	arCOG01589	6.2E−39
SSO2346	Glutathione synthase/glutaminyl transferase/alpha-L-glutamate ligase	arCOG01589	3.3E−37
SSO1223	Catechol 2,3-dioxygenase or other lactoylglutathione lyase family enzyme	arCOG06037	0
SSO2054	Catechol 2,3-dioxygenase or other lactoylglutathione lyase family enzyme	arCOG06037	0
SSO2426	Lactoylglutathione lyase or related enzyme	arCOG02706	5E−24
SSO0192*	Thiol-disulfide isomerase or thioredoxin (SsPDO)	arCOG01218	ref [8]
SSO0314	Predicted thioredoxin/glutaredoxin	arCOG04235	0
SSO3216*	Gamma-glutamyltransferase	arCOG04053	Annotated

SSO0192* has been biochemically characterized and displays activity with GSSG and GSH; SSO3216* is annotated.

genes for putative enzymes were analyzed using machine learning approaches [38,39]. This resulted in the identification of three genes with significant similarity to those of glutathione synthase, a protein disulfide oxidoreductase with experimentally validated GSH-thiol transferase activity [9], and confirmation of a newly annotated gamma-glutamyltransferase (Table 1).

4. Discussion

This report provides evidence from multiple systems that the ratio of oxidized to reduced thiol in *S. solfataricus* is substantially shifted toward the oxidized form. This cellular state does not appear to be maintained by novel pathways or enzymes, but through adjustment of the canonical redox system. Global analysis of intracellular protein disulfide shows that there is a substantial increase in the number of fluorescently labeled proteins after reduction, an observation which contrasts most bacterial and eukaryotic systems [1]. Previous investigations of thiol content in thermophilic organisms reported an absence of glutathione or alternatives, such as γ-glutamylcysteine found in archaea from cooler environments [26,27]. We confirmed the absence of small molecule thiol by chemically labeling reduced thiol in *S. solfataricus* metabolite extracts. However, our large scale metabolomic survey detected glutathione in an oxidized form, GSSG. This result prompted a careful investigation of the *S. solfataricus* genome, in which genes with significant similarity to those involved in glutathione synthesis and regulation were validated. Enzyme assays on protein disulfide oxidoreductase (*Ss*PDO) from *S. solfataricus* show that glutathione (GSH) dependent

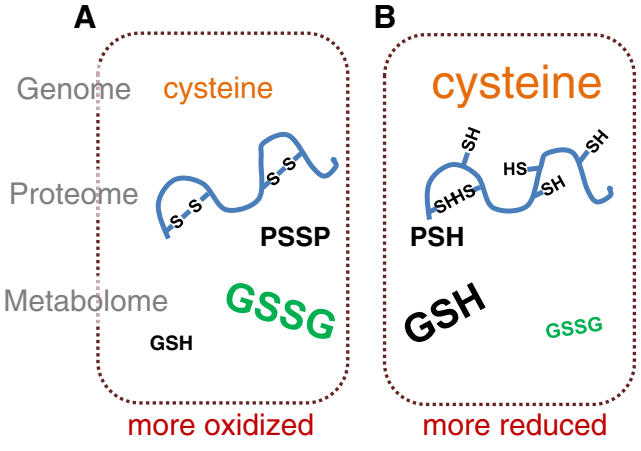

Fig. 3. Results of genomic, proteomic and metabolomic investigation comparing thiol content of the thermophilic *S. solfataricus* (A) to physiologic conditions typically observed in mesophilic organisms (B). Genomic analysis indicates that a reduced amount of the amino acid cysteine is used in the proteins of *S. solfataricus*. Proteomic investigation indicates that cysteines (PSH) in *S. solfataricus* occur primarily as protein disulfides (PSSP) unlike *E. coli*. The ratio of oxidized (GSSG) to reduced glutathione (GSH) is also much higher in *S. solfataricus*. Together, these results suggest a new model for redox homeostasis in thermophilic organisms.

thiol-transferase activity is suppressed [9]. This would help establish/maintain oxidized protein disulfides, because the GSH/GSSG ratio is linked to PSH/PSSP ratio through direct and indirect redox transfer reactions [2]. Connectivity of chemical potential between small molecules and proteins allows cells to take advantage of substantial redox buffering capacity of the protein thiol pool [2–5].

Historically, it was suggested that proteins in archaea were low in cysteine residues and disulfide bonds [40], but more recently evidence shows significant disulfide bonding in thermophilic archaea [11–17]. In the case of *S. solfataricus*, the amount of free thiol in the proteome and metabolome is lower, and the abundance of intracellular protein disulfides are higher than bacterial or eukaryotic model organisms, prompting us to put forth a new thiol-redox strategy (Fig. 3). Many of the proteins from *S. solfataricus* show an absence of cysteine (36.5%), but this is not surprising considering studies of thermophilic viruses which show the membrane proteins often lack any cysteine [15]. Combined with previous results it seems likely that thermophiles utilize a more oxidizing intracellular environment to take advantage of the structural stability imparted by disulfides. To achieve this, thermophilic organisms need to maintain an intracellular environment in which protein disulfides persist. In this case, a glutathione based thiol pool may not be appropriate as a redox buffer. It has been previously suggested that coenzyme A could take on this role, but a lack of detectable levels in this study (Fig. 2C) and others [25] suggests that this is unlikely. An alternative explanation is that *S. solfataricus* has reduced the role of thiol in redox chemistry, freeing disulfides to be used extensively for thermostability of intracellular proteins. Consistent with this model is the fact that while disulfide number is increased, the overall percentage of cysteine residues is reduced because of the potential to form unwanted crosslinks. Previous investigations of the cellular response to oxidative stress lend further support to an alternative cytoplasmic potential. We found that during periods of oxidative stress the gene encoding gamma-glutamyltransferase (Sso3216) is up-regulated, and the putative protein glutathione synthase (Sso0159) is down-regulated in *S. solfataricus*, which would trigger a depletion of the GSH pool [22].

By using an integrated analysis of metabolites and proteins, a unified model of thermophile redox physiology is put-forth. A point that remains to be addressed is the role of glutathione in *S. solfataricus* and whether this represents an ancestral cellular state from a time before reactive oxygen species altered the landscape of biology [41]. A substantial thiol pool exists in mesophilic organisms from all branches of life; even mesophilic archaea utilize a glutathione-like thiol pool [6,26,27]. Based on the placement of thermophilic archaea close to the last universal common ancestor in rRNA phylogenies, we suggest that thiol-based systems now used for maintaining a reducing intracellular environment are derived from metabolic pathways originally tasked with keeping protein disulfide bonds intact at high temperature.

Acknowledgements

The authors thank Edward Schmidt for helpful comments on the manuscript, Susan K. Brumfield for SEM images in Graphic Abstract,

Lakshindra Chetia for synthesis of ZB-M LC-01-56, Merrill Oakley and Michelle Tigges for the work with metabolite extractions, and Rebecca Sorenson and Sophia Froelich for the help with bioinformatics. This work was supported by National Science Foundation, MCB0646499 and MCB102248. Mass Spectrometry, Proteomics and Metabolomics core facility was supported by the Murdock Charitable Trust, INBRE MT Grant No. P20 RR-16455-08, NIH Grant Nos. P20 RR-020185 and P20 RR-024237 from the COBRE Program of the National Center for Research Resources.

Appendix A. Supplementary data

Supplementary data to this article can be found online at http://dx.doi.org/10.1016/j.bbagen.2013.08.009.

References

[1] C.S. Sevier, C. Kaiser, Formation and transfer of disulphide bonds in living cells, Nat. Rev. Mol. Cell Biol. 3 (2002) 836–847.
[2] R.E. Hansen, D. Roth, J.R. Winther, Quantifying the global cellular thiol-disulfide status, Proc. Natl. Acad. Sci. U. S. A. 106 (2009) 422–427.
[3] R.C. Cumming, N.L. Andon, P.A. Haynes, P. Minkyu, D. Schubert, Protein disulfide bond formation in the cytoplasm during oxidative stress, J. Biol. Chem. 279 (2004) 21749–21758.
[4] S. Chakravarthi, C.E. Jessop, N.J. Bulleid, The role of glutathione in disulphide bond formation and endoplasmic-reticulum-generated oxidative stress, EMBO Rep. 7 (2006) 271–275.
[5] A. Pastore, G. Federici, E. Bertini, F. Piemonte, Analysis of glutathione: implication in redox and detoxification, Clin. Chim. Acta 333 (2003) 19–39.
[6] R.C. Fahey, Novel thiols of prokaryotes, Annu. Rev. Microbiol. 55 (2001) 333–356.
[7] G.V. Smirnova, O.N. Oktyabrsky, Glutathione in bacteria, Biochemistry, Biokhimiia 70 (2005) 1199–1211.
[8] M. Fratelli, Gene expression profiling reveals a signaling role of glutathione in redox regulation, Proc. Natl. Acad. Sci. U. S. A. 102 (2005) 13998–14003.
[9] E. Pedone, D. Limauro, R. D'Alterio, M. Rossi, S. Bartolucci, Characterization of a multifunctional protein disulfide oxidoreductase from *Sulfolobus solfataricus*, FEBS J. 273 (2006) 5407–5420.
[10] I. Derman, J. Beckwith, *Escherichia coli* alkaline phosphatase fails to acquire disulfide bonds when retained in the cytoplasm, J. Bacteriol. 173 (1991) 7719–7722.
[11] P. Mallick, D.R. Boutz, D. Eisenberg, T.O. Yeates, Genomic evidence that the intracellular proteins of archaeal microbes contain disulfide bonds, Proc. Natl. Acad. Sci. U. S. A. 99 (2002) 9679–9684.
[12] M. Beeby, B.D. O'Connor, C. Ryttersgaard, D. Boutz, T.O. Yeates, The genomics of disulfide bonding and protein stabilization in thermophiles, PLoS Biol. 3 (2005) e309.
[13] J. Jorda, T.O. Yeates, Widespread disulfide bonding in proteins from thermophilic archaea, Archaea (2011) 409156.
[14] Q. She, R.K. Singh, F. Confalonieri, Y. Zivanovic, J. van der Oost, The complete genome of the crenarchaeon *Sulfolobus solfataricus* P2, Proc. Natl. Acad. Sci. U. S. A. 98 (2001) 7835–7840.
[15] S.K. Menon, W.S. Maaty, G.J. Corn, B. Bothner, C.M. Lawrence, Cysteine usage in *Sulfolobus* spindle-shaped virus 1 and extension to hyperthermophilic viruses in general, Virology 376 (2008) 270–278.
[16] E.T. Larson, B. Eilers, S. Menon, D. Reiter, C.M. Lawrence, A winged-helix protein from Sulfolobus turreted icosahedral virus points toward stabilizing disulfide bonds in the intracellular proteins of a hyperthermophilic virus, Virology 368 (2007) 249–261.
[17] C.M. Lawrence, S. Menon, B.J. Eilers, B. Bothner, R. Khayat, T. Douglas, M.J. Young, Structural and functional studies of archaeal viruses, J. Biol. Chem. 284 (2009) 12599–12603.
[18] C.E. Nunn, U. Johnsen, P. Schonheit, T. Fuhrer, M.J. Danson, Metabolism of pentose sugars in the hyperthermophilic archaea *Sulfolobus solfataricus* and *Sulfolobus acidocaldarius*, J. Biol. Chem. 285 (2010) 33701–33709.
[19] H.J. Lamble, A. Theodossis, C.C. Milburn, G.L. Taylor, M.J. Danson, Promiscuity in the part-phosphorylative Entner–Doudoroff pathway of the archaeon *Sulfolobus solfataricus*, FEBS Lett. 579 (2005) 6865–6869.
[20] S.V. Albers, N. Birkeland, A.J. Driessen, S. Gertig, M. Zaparty, SulfoSYS (Sulfolobus Systems Biology): towards a silicon cell model for the central carbohydrate metabolism of the archaeon *Sulfolobus solfataricus* under temperature variation, Biochem. Soc. Trans. 37 (2009) 58–64.
[21] J. Heinemann, W.S. Maaty, G.H. Gauss, N. Akkaladevi, B. Bothner, Fossil record of an archaeal HK97-like provirus, Virology 417 (2011) 362–368.
[22] W.S. Maaty, B. Bothner, Something old, something new, something borrowed; how the thermoacidophilic archaeon *Sulfolobus solfataricus* responds to oxidative stress, PLoS One 4 (2009) e6964.
[23] W.S. Maaty, K. Selvig, S. Ryder, P. Tarlykov, J.K. Hilmer, J. Heinemann, J. Steffens, J.C. Snyder, A.C. Ortmann, N. Movahed, K. Spicka, L. Chetia, P.A. Grieco, E.A. Dratz, T. Douglas, M.J. Young, B. Bothner, Proteomic analysis of *Sulfolobus solfataricus* during Sulfolobus Turreted Icosahedral Virus infection, J. Proteome Res. 11 (2012) 1420–1432.
[24] W.S. Maaty, J.D. Steffens, J. Heinemann, A.C. Ortmann, B.D. Reeves, S.K. Biswas, E.A. Dratz, P.A. Grieco, M.J. Young, B. Bothner, Global analysis of viral infection in an archaeal model system, Front. Microbiol. 3 (2012) 411.
[25] C.S. Hummel, K.M. Lancaster, J. Edward, E.J. Crane, Determination of coenzyme A levels in *Pyrococcus furiosus* and other Archaea: implications for a general role for coenzyme A in thermophiles, FEMS Microbiol. Lett. 252 (2005) 229–234.
[26] N. Allocati, L. Federici, M. Masulli, C. Di Ilio, Distribution of glutathione transferases in Gram-positive bacteria and Archaea, Biochimie 94 (2012) 588–596.
[27] L. Malki, M. Yanku, Y. Borovok, G. Cohen, Y. Aharonowitz, Identification and characterization of gshA, a gene encoding the glutamate-cysteine ligase in the halophilic archaeon *Haloferax volcanii*, J. Bacteriol. 191 (2009) 5196–5204.
[28] B. Wiedenheft, J. Mosolf, D. Willits, M. Yeager, K.A. Dryden, M. Young, T. Douglas, An archaeal antioxidant: characterization of a Dps-like protein from *Sulfolobus solfataricus*, Proc. Natl. Acad. Sci. U. S. A. 102 (2005) 10551–10556.
[29] W.S. Rasband, ImageJ, U.S. National Institutes of Health, Bethesda, Maryland, USA, 2012. (Available at: http://rsbweb.nih.gov/ij/).
[30] A.B. Canelas, A. Pierick, C. Ras, R.M. Siefar, J.J. Heijnen, Quantitative evaluation of intracellular metabolite extraction techniques for yeast metabolomics, Anal. Chem. 81 (2009) 7379–7389.
[31] O. Yanes, R. Tautenhahn, G.J. Patti, G. Siuzdak, Expanding coverage of the metabolome for global metabolite profiling, Anal. Chem. 83 (2011) 2152–2161.
[32] R. Tautenhahn, C. Böttcher, S. Neumann, Highly sensitive feature detection for high resolution LC/MS, BMC Bioinformatics 9 (2008) 504.
[33] C. Smith, G. O'Maille, E.J. Want, C. Qin, G. Siuzdak, METLIN: a metabolite mass spectral database, Ther. Drug Monit. 27 (2005) 747–751.
[34] G.J. Patti, R. Tautenhahn, G. Siuzdak, Meta-analysis of untargeted metabolomic data from multiple profiling experiments, Nat. Protoc. 7 (2012) 508–516.
[35] G.J. Patti, R. Tautenhahn, D. Rinehart, K. Cho, L.P. Shriver, M. Manchester, I. Nikolskiy, C.H. Johnson, N.G. Mahieu, G. Siuzdak, A view from above: cloud plots to visualize global metabolomic data, Anal. Chem. 85 (2013) 798-04.
[36] R. Tautenhahn, G.J. Patti, D. Rinehart, G. Siuzdak, XCMS online: a web-based platform to process untargeted metabolomic data, Anal. Chem. 84 (2012) 5035–5039.
[37] E.F. Pai, G.E. Schulz, The catalytic mechanism of glutathione reductase as derived from x-ray diffraction analyses of reaction intermediates, J. Biol. Chem. 258 (1983) 1752–1757.
[38] M. Dlakić, HHsvm: fast and accurate classification of profile–profile matches identified by HHsearch, Bioinformatics 25 (2009) 3071–3076.
[39] A.R. Shah, C.S. Oehmen, B. Webb-Robertson, SVM-HUSTLE—an iterative semi-supervised machine learning approach for pairwise protein remote homology detection, Bioinformatics 24 (2008) 783–790.
[40] R. Ladenstein, B. Ren, Reconsideration of an early dogma, saying "there is no evidence for disulfide bonds in proteins from archaea", Extremophiles 12 (2008) 29–38.
[41] D. Schwartzman, C.H. Lineweaver, Biospheric self-organization a hyperthermophilic origin of life, in: A. Kleidon, R.D. Lorenz (Eds.), Non-Equilibrium Thermodynamics and the Production of Entropy, Springer-Verlag Berlin Heidelberg, Germany, 2005, pp. 207–221.